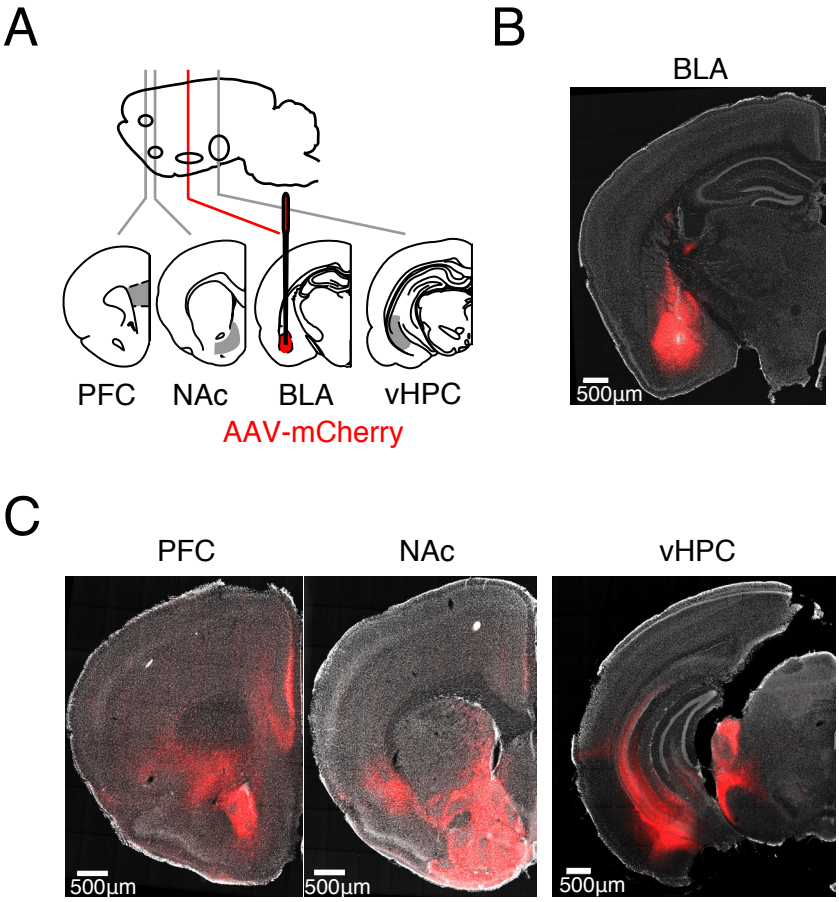

Figure S1. BLA axons project to multiple targets, Related to Figure 1.

A) AAV-mCherry injection into the BLA to label axons in the PFC, NAc and vHPC.

B) Injection site in the BLA, with DAPI staining in grey.

C) BLA axons (red) in the PFC (*left*), NAc (*middle*) and vHPC (*right*).

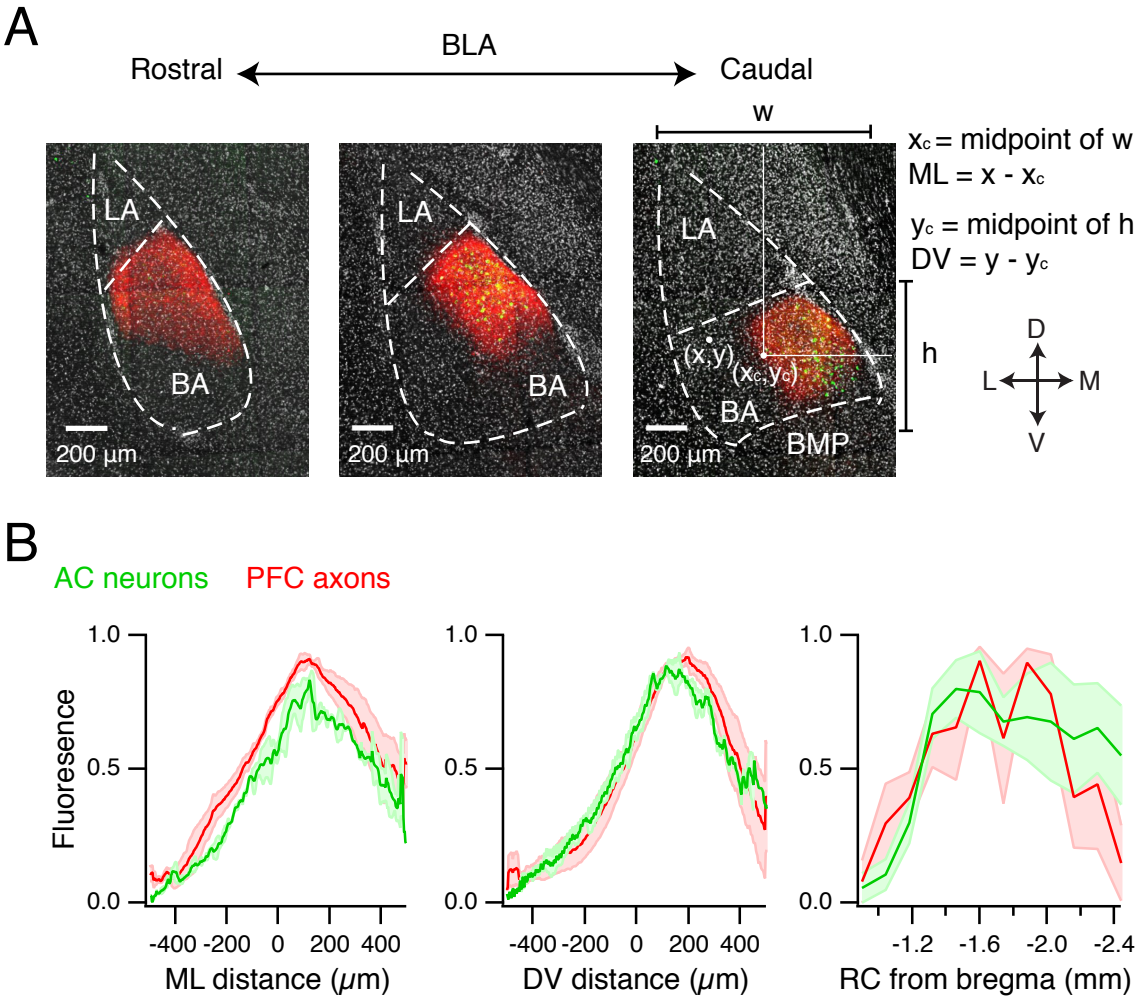

Figure S2. PFC axons and AC neurons overlap in the BLA, Related to Figure 1.

A) *Left,* PFC axons (red) and AC neurons (green) in rostral to caudal sections of the BLA, with DAPI in grey. *Right,* Coordinate system and calculation of the medial-lateral (ML) and dorsal-ventral (DV) locations.

B) Fluorescence profiles of AC neurons (green) and PFC axons (red) along the ML axis (*left*), DV axis (*middle*) and rostral-caudal (RC) axis (*right*). (n = 3 animals)

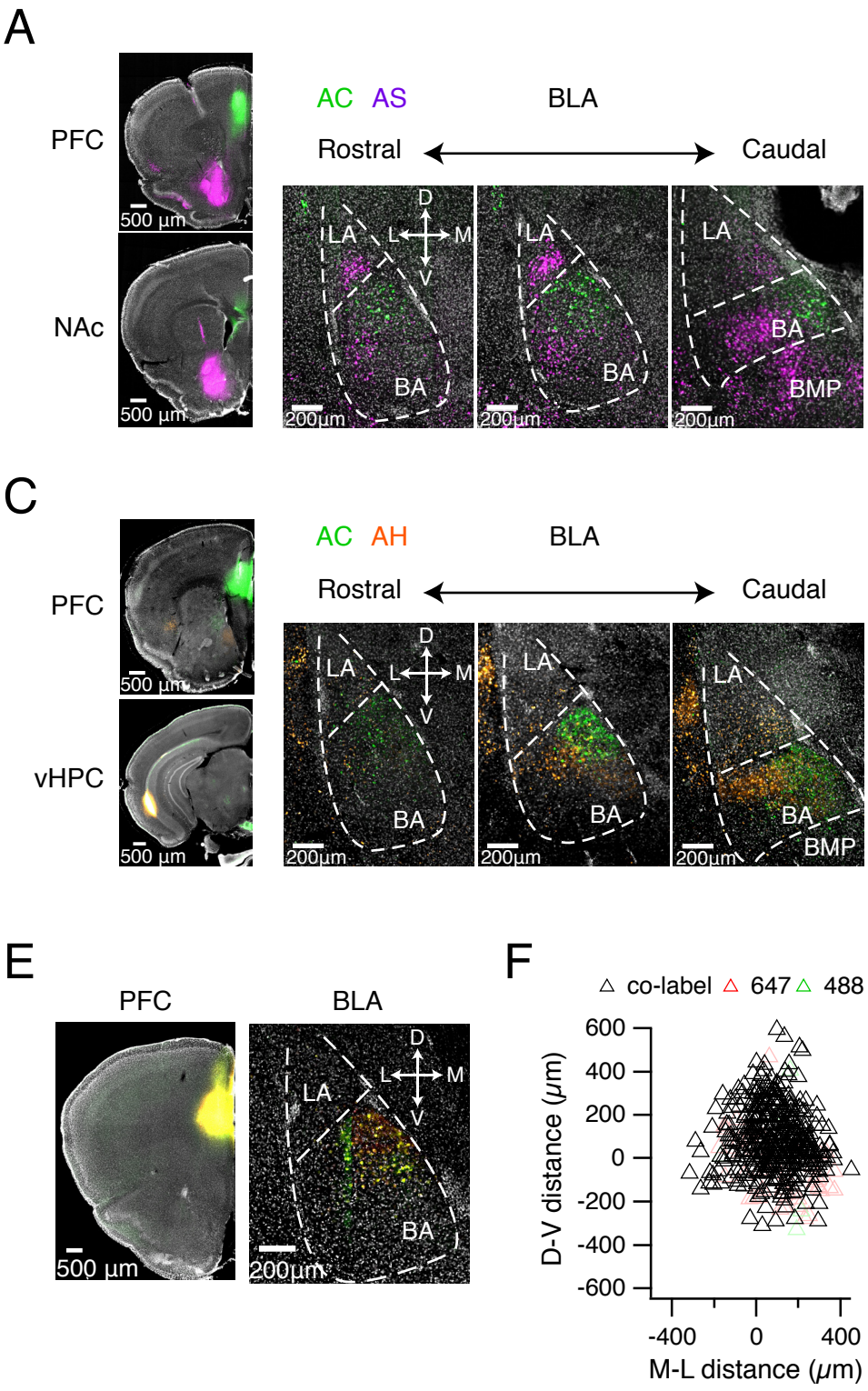
A
PFC
NAc
500 µm
AC AS
BLA
Rostral
Caudal
D
L
M
V
LA
BA
BMP
200µm
B
co-label AC AS
DV distance (µm)
ML distance (µm)
C
AC AH
vHPC
D
co-label AC AH
E
PFC
BLA
F
co-label 647 488
D-V distance (µm)
M-L distance (µm)
G
Percent co-labeled cells
AC AS
AC AH
AC AC

Figure S3. Distinct topography of BLA projection neurons, Related to Figure 1.

A) *Left*, CTB-488 injection site in the PFC (*top*) and CTB-647 injection site in the NAc (*bottom*). *Right*, AC (green) and AS (purple) neurons in rostral to caudal sections of the BLA, with DAPI in grey.

B) ML (x-axis) and DV (y-axis) locations of AC (green) and AS (purple) neurons. Black triangles indicate co-labeled neurons, and solid triangles indicate mean locations. (n = 3 animals)

C) Similar to (A) for AC (green) and AH (orange) neurons.

D) Similar to (B) for AC (green) and AH (orange) neurons. (n = 3 animals)

E) *Left,* CTB-488 and CTB-647 injection site in the PFC. *Right*, AC neurons labeled by CTB-488 (green) and CTB-647 (red).

F) ML (x-axis) and DV (y-axis) locations of co-labeled (black) and single labeled (green and red) neurons in the BLA. (n = 3 animals)

G) Percent of co-labeled cells, as a function of all labeled cells, for dual CTB injections in two brain regions or the same brain region listed along the x axis.

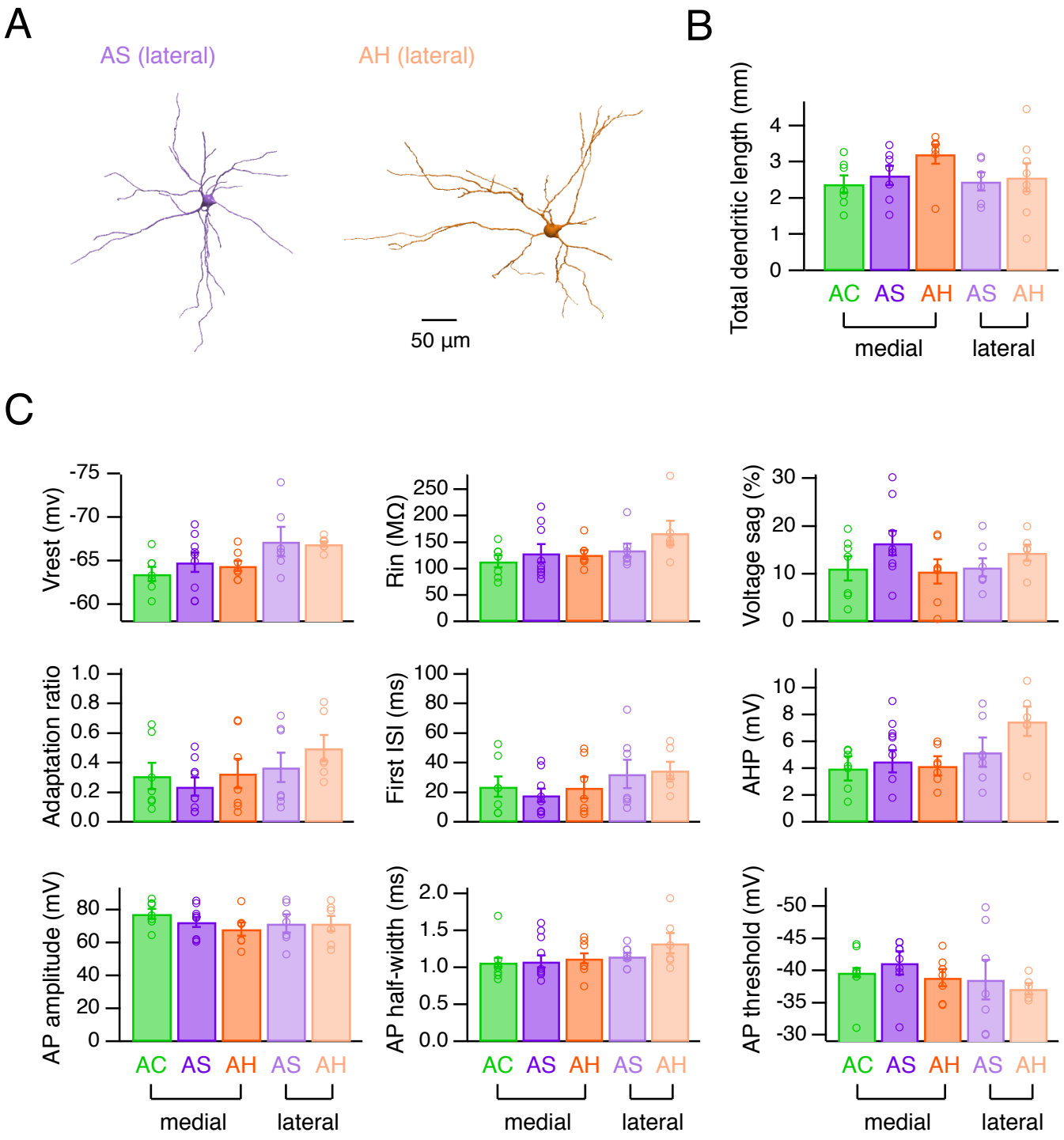

Figure S4. Properties of different BLA projection neurons, Related to Figures 2 &4.

A) Reconstruction of AS and AH neurons located in the lateral BLA.

B) Summary of total dendritic length at five projection neuron populations in the BLA (AC: n = 7 cells; AS medial: n = 7 cells; AH medial: n = 7 cells; AS lateral: n = 7 cells; AH lateral: n = 7 cells).

C) Summary of passive, firing and single AP properties at the different projection neurons (AC: n = 7 cells; AS medial: n = 9 cells; AH medial: n = 7 cells; AS lateral: n = 7 cells; AH lateral: n = 7 cells).

SUPPLEMENTAL EXPERIMENTAL PROCEDURES

Experiments were performed using P42-P56 male mice in a C57 BL/6J background. All procedures followed guidelines approved by the New York University Animal Welfare Committee.

Stereotaxic Injections

To target different neurons and connections, stereotaxic injections were performed on P28-P36 mice, as described previously (Little and Carter, 2012). Injection site coordinates were (relative to bregma for mediolateral axis, dorsoventral axis, and rostrocaudal axis: prelimbic PFC = -0.3 mm, -2.3 mm, and +2.1 mm; NAc = -2.6 mm, -4.6 mm, +1.7 mm at 13°; BLA = -3 mm, -5 mm, and -1.3 mm; vHPC = -3.3 mm, -3.6 / -4.2 mm, and -3 mm). For anterograde tracing, 147-202 nl of virus was injected (AAV2/1-hSyn-GFP or AAV2/1-CB7-mCherry; UPenn Vector Core). For retrograde labeling, 147-184 nl of a 0.2% dilution of Alexa-conjugated Cholera Toxin subunit B (CTB-Alexa 488 or CTB-Alexa 647; Invitrogen) or undiluted retrobeads (green or red; Lumafluor) was injected. To eliminate recording biases, the color used to label each projection neuron was alternated across experiments. For combined retrograde labeling and optogenetics, 276-368 nl of a 2:1 mixture of virus (AAV2/1-hSyn-hChR2-eYFP; UPenn Vector Core) and either red or green retrobeads was injected. After all injections, animals were returned to their home cages for 2-3 weeks to allow for expression and transport before being used for experiments.

Slice Preparation

Mice were anesthetized with an intraperitoneal injection of a lethal dose of ketamine / xylazine. After anesthesia, mice were perfused intracardially with an ice-cold solution containing the following (in mM): 65 sucrose, 76 NaCl, 25 $NaHCO_3$, 1.4 NaH_2PO_4, 25 glucose, 2.5 KCl, 7 $MgCl_2$, 0.4 Na-ascorbate, and 2 Na-pyruvate (bubbled with 95% O_2/5% CO_2). Coronal sections (300 μm thick) of the BLA were cut in this solution and transferred to artificial CSF (ACSF) containing the following (in mM): 120 NaCl, 25 $NaHCO_3$, 1.4 NaH_2PO_4, 21 glucose, 2.5 KCl, 2 $CaCl_2$, 1 $MgCl_2$, 0.4 Na-ascorbate, and 2 Na-pyruvate (bubbled with 95% O_2/5% CO_2). Coronal sections were also cut from the injection site(s), which were validated for accuracy and slices were discarded from animals with off-target injection site(s). Slices were recovered for 30 min at 34°C and then stored for at least 30 min at 24°C. All experiments were conducted at 31 - 34°C. In many experiments, 1 μM TTX, 0.1 mM 4-AP and elevated Ca2+ (4 mM) were included to block action potentials (APs) and restore presynaptic glutamate release, respectively (Little and Carter, 2012; Petreanu et al., 2009). In some experiments, one or more of the following were bath-applied: 10 μM NBQX to block AMPA-Rs, 10 μM CPP to block NMDA-Rs, 10 μM D-serine to allow NMDA-R activation, 10 μM gabazine to block $GABA_A$-Rs, 5 μM CGP to block $GABA_B$-Rs. In experiments examining asynchronous release events, extracellular calcium was replaced with strontium (4 mM). All chemicals were from Sigma or Tocris Bioscience.

Electrophysiology

Targeted recordings were made from neurons in the BLA using infrared-differential interference contrast (IR-DIC). Amygdala-cortical (AC), amygdala-hippocampal (AH) and amygdala-striatal (AS) neurons were identified by the presence of red or green retrobeads. Unless otherwise specified, neurons were targeted in the medial part of the BLA where all three cell types are found. Recording order was alternated across experiments for the two cell types in each pair of compared neurons. For voltage-clamp experiments, borosilicate pipettes (3-5 MΩ) were filled with (in mM): 135 Cs-gluconate, 10 HEPES, 10 Na-phosphocreatine, 2 Mg_2-ATP, 0.4 NaGTP, 10 TEA, 2 QX-314, and 10 EGTA, pH 7.3 with CsOH (290-295 mOsm). For current-clamp recordings, borosilicate pipettes (3-5 MΩ) were filled with (in mM): 135 K-gluconate, 7 KCl, 10 HEPES, 10 Na-phosphocreatine, 4 Mg_2-ATP, 0.4 NaGTP, and 0.5 EGTA, pH 7.3 with KOH (290-295 mOsm). In some experiments, 30 μM Alexa Fluor 594 or 488 were added to visualize neuronal morphology with 2-photon microscopy. Physiology data were collected with a Multiclamp 700B amplifier. Signals were sampled at 10 kHz and filtered at 5 kHz for current-clamp recordings and at 2 kHz for voltage-clamp recordings. Series resistance was <25 MΩ and not compensated.

Optogenetics

Glutamate release was triggered by activating channelrhodopsin-2 (ChR2) present in the presynaptic terminals of PFC inputs to the BLA, in a manner previously described (Little and Carter, 2012). In optogenetic experiments, nearby AC:AS pairs or AC:AH pairs were recorded in random order. ChR2 was activated with 0.5-8 ms pulses of 473 nm light from a light-emitting diode (LED) through a 10x objective using a power of ~3 mW.

Two-photon microscopy

Two-photon imaging was performed on a custom microscope, as previously described (Chalifoux and Carter, 2010). Briefly, a titanium:sapphire laser (Coherent) tuned to 810 nm was used to excite Alexa Fluor 594 or 488 to image dendrite morphology. Imaging was performed with a 60x 1.0 NA objective (Olympus).

Histology

Mice were anesthetized and perfused intracardially with 0.01 M PBS and 4% PFA. Brains were stored in 4% PFA for 12-18 h at 4°C before being transferred to 0.01 M PBS. Slices were cut on a VT-1000S vibratome (Leica) at 70 µm thickness and placed on gel-coated glass slides. ProLong Gold anti-fade reagent with DAPI (Invitrogen) or Vectashield with DAPI (Vector Labs) was applied to the slide, which was then covered with a glass coverslip. Fluorescent images were taken on an Olympus VS120 microscope with a 10x objective.

Data analysis

Imaging and physiology data were acquired using National Instruments boards and custom software written in MATLAB (MathWorks). Image processing and analysis was performed in NIH ImageJ. Physiology analysis was performed in Igor Pro (Wavemetrics). Morphological reconstructions were performed in NeuronStudio (Wearne et al., 2005). Statistical analysis was performed in Prism 7.0 (GraphPad).

Axon and projection neuron distributions along the rostro-caudal axis were calculated using images between -0.9 to -2.4 mm from bregma in 140 µm steps. Images were aligned with the "Register Virtual Stack Slices" plugin in ImageJ, using similarity feature extraction and rigid transformation with no shrinkage, followed by transforms applied to the channels containing the fluorescence signals. The fluorescence intensity profile along the z-axis of the aligned image stack was minimum subtracted, and then normalized to the maximum intensity across the slices. Axon distribution along the mediolateral and dorsoventral axes was measured from images between -1.18 and -2.16 mm rostro-caudal from bregma in 140 µm steps, with distance quantified relative to the center of the BLA in each slice. The fluorescence intensity profiles were minimum subtracted, and then normalized to the maximum in each slice. For co-localization of retrogradely labeled neurons, cell counting was performed in ImageJ on a 3-color image of AC:AS, AC:AH or AC:AC neurons with DAPI labeling. All CTB-labeled cell bodies in the BLA were manually counted across 3 slices, corresponding to -1.3, -1.6 and -1.9 mm rostro-caudal to bregma per animal. Location was quantified relative to the center of the BLA in each slice. For analysis of morphology, the dendrites of Alexa-filled neurons were reconstructed in NeuronStudio from two-photon image stacks, as previously described (Little and Carter, 2013).

Intrinsic physiology was assessed from 500 ms current steps in 50 pA increments from 50 to 250 pA and -50 pA. Input resistance was calculated from the steady-state voltage during a -50 pA current step. Voltage sag was also calculated from this response as $(V_{sag}-V_{ss}) / (V_{sag}-V_{baseline})$, where V_{sag} is the average over a 1 ms window around the minimum peak, V_{ss} is the average of the last 50 ms, and $V_{baseline}$ is the average of the 50 ms preceding the current injection. Firing adaptation was calculated as the ratio of the first and last inter-spike intervals, such that a value of 1 indicates no adaptation and values less than 1 indicate lengthening of the inter-spike interval, measured from responses to the current step that gave a range of 5-10 AP. First inter-spike interval and single AP properties were determined from the first current step that elicited firing. AP threshold was defined as the voltage at which dV / dt exceeds 10 mV / ms. AP half-width was measured at the mid-point of threshold and peak. AP amplitude was measured as the difference between threshold and peak. Afterhyperpolarization (AHP) was measured as the difference between the inflection

point of the AP on the falling phase and threshold voltage. Current-clamp recordings are shown in figures as representative examples, with individual traces for suprathreshold responses and average for subthreshold responses.

EPSC amplitudes were calculated as the average within a ± 1 ms window surrounding the peak response. NMDA-R EPSCs were calculated as the peak of the +40 mV EPSC at 50 ms after onset, at which time the AMPA-R component has decayed. Average EPSCs are shown in figures as mean ± SEM of all recorded neurons for each experiment. Detection of qEPSCs were performed with the NeuroMatic plugin for Igor Pro, using a threshold detection algorithm with an onset search of 2 standard deviations below a 5 ms sliding window average and minimum event size of 5 pA. Baseline events were detected in the 600 ms preceding light stimulation and evoked events were detected in the 10-600 ms after the stimulus. To quantify the frequency of PFC evoked qEPSCs independent of baseline frequency, Δ frequency was compared between paired neurons, equal to the difference between baseline and post-stimulation frequency.

Summary comparisons show arithmetic mean ± SEM, except for cell type ratio (AS / AC and AH / AC) data shown as geometric mean ± 95% confidence interval. Statistical comparisons of measured values between 2 groups were performed using the non-parametric Mann-Whitney test if data were not acquired in pairs, or using the non-parametric Wilcoxon Signed-Rank test if data were acquired in pairs. Statistical comparisons of measured values between more than 2 groups were performed using the non-parametric Kruskal-Wallis test, followed by Dunn's test for post-test evaluation of significant interactions. Statistical comparisons of measured values across multiple variables (for example, AP firing over a range of current steps) were performed using two-way ANOVA with Sidak's test for multiple comparisons. Two-tailed p values < 0.05 were considered significant.

SUPPLEMENTAL REFERENCES

Chalifoux, J.R., and Carter, A.G. (2010). GABAB receptors modulate NMDA receptor calcium signals in dendritic spines. Neuron *66*, 101-113.